6th European Conference on Computational Mechanics (ECCM 6)
7th European Conference on Computational Fluid Dynamics (ECFD 7)
1115 June 2018, Glasgow, UK

UNCERTAINTY QUANTIFICATION AND ROBUST DESIGN FOR AERODYNAMIC APPLICATIONS USING CONTINUOUS ADJOINT METHODS

Anastasios K. Papageorgiou[1], Kimon B. Fragkos[1], Evangelos M. Papoutsis-Kiachagias[1] and Kyriakos C. Giannakoglou[1]

[1] National Technical University of Athens (NTUA), School of Mechanical Engineering, Parallel CFD & Optimization Unit, Athens, Greece,
e-mail: tkpapageorgiou@gmail.com, kimonfragos@gmail.com, vaggelisp@gmail.com, kgianna@central.ntua.gr

Key words: *Uncertainty Quantification, Robust Design, Method of Moments, Intrusive Polynomial Chaos Expansion, Continuous Adjoint Methods*

Abstract. In CFD-based applications, propagating uncertainties associated with the operating conditions or shape imperfections from the system input to its output, a.k.a. uncertainty quantification (UQ), and optimization under uncertainties (robust design) are at the cutting edge of research. In gradient-based robust design, the computation of the gradient of an objective function which accounts for all uncertainties is required. In this paper, two UQ methods are developed and presented; the first one is based on the Method of Moments (MoM, [6]) whereas the second on the intrusive Polynomial Chaos Expansion (iPCE), both for incompressible fluid flows. Regarding optimization, a combination of the mean value and standard deviation of a quantity of interest (QoI, for instance drag or lift) forms the objective function to be minimized; in this paper, a gradient-based method, supported by the continuous adjoint, is used to minimize it. The adjoint to both UQ methods is presented. The iPCE-based method requires the development and validation of the adjoint to the iPCE PDEs. With the first-order variant of the MoM, the objective function includes the first derivatives of the QoI with respect to (w.r.t.) the uncertain variables which are then differentiated w.r.t. the design variables to minimize it. To avoid costly computations, this paper proposes the computation of projections of the second-order mixed derivatives to vectors, instead of the Hessian matrix itself. A combination of the continuous adjoint and direct differentiation can efficiently compute this projection, leading to an overall cost per optimization cycle that is independent of the number of both the uncertain and the design variables. For the purpose of demonstration, the flow problem around an isolated airfoil is studied with all methods; the validation of the computed derivatives is presented.

1 Introduction

Most shape optimization techniques consider all inputs known with absolute certainty. As a result, the solution optimality refers exclusively to a single operating point. However, in real problems, the environmental conditions may vary within a certain range. These varying conditions are usually referred to as uncertain variables and follow a certain statistical distribution (normal, Weibull etc.) which is either known or assumed to be known; these distributions are expressed through their mean values and standard deviations. Therefore, there is a need to develop UQ tools in order to propagate flow uncertainties from the system input to its output; the latter is, herein, referred to as the QoI and is, practically, the one that would have been optimized in the absence of uncertainties. In case the target is to optimize an aerodynamic shape by also considering uncertainties, the new objective function should be expressed in terms of the mean value and standard deviation of the QoI. Usually, combining the first two statistical moments of the QoI is enough. In case of a gradient-based optimization method, the gradient of the so-defined objective function w.r.t. the design variables should be computed, too.

Some methods that are often used to propagate uncertainties are the Monte-Carlo (MC) or Quasi-MC ([3]), MoM ([6]) and Polynomial Chaos Expansion ones (PCE, [1],[8]). The latter appears in two variants, namely the intrusive and the non-intrusive one. All methods based on MC techniques are straightforward and demand a considerably high number of CFD evaluations which make them unaffordable. This paper presents the mathematical formulation and assessment of iPCE and MoM, which both have a significantly lower computational cost than MC. The computed mean values and standard deviations of the QoI are firstly validated against MC. Next step is to proceed to the optimization of an objective function built by concatenating the mean value and standard deviation of the QoI. The optimization runs are performed using gradient-based methods supported by the continuous adjoint. Although PCE has been frequently used during the last years ([2], [1], [8]), the continuous adjoint to the iPCE PDEs for laminar, incompressible flows is presented for the first time in the literature. The advantage of iPCE compared to the non-intrusive approach is that the former is more accurate ([7]); hence, a lower chaos order can be used to obtain the same level of accuracy, at a lower cost. Regarding the optimization with the first-order variant of the MoM, an idea borrowed from truncated Newton methods ([4]) is used to avoid the computation of second-order derivatives; instead, their projections to certain vectors are computed at a much lower CPU cost. This will be referred to as the projected First-Order-Second-Moment (pFOSM) method.

2 Primal Equations, QoI and Objective Function

The governing equations are the steady state Navier-Stokes PDEs, for 2D laminar flows of an incompressible fluid,

$$\begin{aligned} R^p &= -\frac{\partial v_j}{\partial x_j} = 0 \\ R_i^v &= v_j \frac{\partial v_i}{\partial x_j} - \frac{\partial \tau_{ij}}{\partial x_j} + \frac{\partial p}{\partial x_i} = 0, \quad i = 1, 2 \end{aligned} \tag{1}$$

where v_i are the velocity components, $\tau_{ij} = \nu \left(\frac{\partial v_i}{\partial x_j} + \frac{\partial v_j}{\partial x_i} \right)$ the stress tensor components, p the static pressure divided by the fluid density and ν the kinematic viscosity of the fluid. The Einstein notation is used, according to which twice repeated indices imply summation.

Without loss in generality, the drag force

$$F = \int_{S_w} (p\delta_i^j - \tau_{ij}) n_j r_i dS \tag{2}$$

is the QoI throughout this paper, where r_i is the farfield velocity direction. The objective function to be minimized in the optimization under uncertainties is the weighted linear combination of the mean value (μ_F) and standard deviation (σ_F) of the QoI

$$J = w_0 \mu_F + w_1 \sigma_F \tag{3}$$

where w_0, w_1 are weights defined by the designer.

3 Uncertainty Quantification (UQ)

3.1 Method of Moments (MoM)

According to the method of statistical moments, the mean value and standard deviation of the QoI w.r.t. the uncertain variables $c_i, i \in [1, M]$, can be written, by taking into account only the first-order Taylor expansion term (First-Order-Second-Moment, FOSM) ([6]), as

$$\mu_F(c) = F|_{\bar{c}}, \qquad \sigma_F(c) = \sqrt{\sum_{\mu=1}^{M} \left[\frac{\delta F}{\delta c_\mu} \right]_{\tilde{c}}^2 \sigma_\mu^2} \tag{4}$$

From eq. (4), it can be seen that in the FOSM, the mean value of the QoI is not taking the standard deviation of $\vec{c}$ into consideration and is computed at its mean value; this is not true, however, for the standard deviation of the QoI. Apart from the flow field, the computation of J requires the first-order derivatives of the QoI w.r.t. the uncertain variables which are computed using the continuous adjoint method. According to [5], the adjoint equations read

$$\begin{aligned} R^q &= -\frac{\partial u_j}{\partial x_j} = 0 \\ R_i^u &= u_j \frac{\partial v_j}{\partial x_i} - \frac{\partial (v_j u_i)}{\partial x_j} - \frac{\partial \tau_{ij}^a}{\partial x_j} + \frac{\partial q}{\partial x_i} = 0, \quad i = 1, 2 \end{aligned} \tag{5}$$

where u_i are the adjoint velocity components, q the adjoint pressure and τ_{ij}^a the adjoint stress tensor. The adjoint boundary conditions are omitted in the interest of space.

In this paper, uncertainties are associated with the flow conditions and, in specific, the only uncertain variable is the free-stream flow angle $a_\infty = c_\mu = c_1$; this is enough for demonstrating the proposed methods. After satisfying the adjoint PDEs and their

boundary conditions, the gradient of F w.r.t. c_μ is computed through an integral along the inlet boundary S_I as follows

$$\frac{\delta F}{\delta c_\mu} = \int_{S_I} \left[\nu \left(\frac{\partial u_i}{\partial x_j} + \frac{\partial u_j}{\partial x_i} \right) n_j - q n_i \right] \frac{\delta v_i}{\delta c_\mu} dS \tag{6}$$

The $\delta v_i / \delta c_\mu$ term is computed analytically. It is assumed that the solution of the adjoint equations costs as much as that of the flow equations. Each of the primal and adjoint fields is computed at the cost of one Equivalent Flow Solution (EFS). Thus, with the FOSM approach, the computational cost for UQ is 2 EFS, irrespective of the value of M.

3.2 The iPCE Method

According to the PCE method, each uncertain flow variable (e.g. pressure, velocity, etc.) is expressed as the sum of the products of PCE fields $p_l(\vec{x})$ and orthogonal polynomials $H_l(\vec{\xi})$. For example, for the pressure p,

$$p(\vec{x}, \vec{\xi}) = \sum_{l=0}^{L-1} p_l(\vec{x}) H_l(\vec{\xi}) \tag{7}$$

where $\vec{\xi}$ is the vector of uncertain variables. The total number L of terms in the above summation depends on M and the chaos order γ and is equal to $L = \frac{(M+\gamma)!}{M!\gamma!}$. The higher the chaos order, the more accurate the UQ, at the expense though of a higher computational cost. In this paper, a normal distribution is assumed for each uncertain variable and, this is why, H_l stands for the Hermite polynomials.

In intrusive PCE, the expansions of the (uncertain) flow fields (eq. (7)) are introduced to the governing equations; therefore, new PDEs are derived through Galerkin projections. The Galerkin projection of any orthogonal polynomial is defined as $\langle H_i, H_j \rangle = \int H_i(\vec{\xi}) H_j(\vec{\xi}) w(\vec{\xi}) d\vec{\xi}$, where $w(\vec{\xi})$ is the product of the probability density functions (PDF) of the distributions of all uncertain variables. By making use of the properties of Galerkin projections, L systems of PDEs similar to the Navier-Stokes equations are derived. The new set of PDEs is

$$\begin{aligned} {}^l R^p &= -\frac{\partial v_{im}}{\partial x_i} \langle H_m, H_l \rangle = 0 \\ {}^l R^v_i &= v_{jm} \frac{\partial v_{is}}{\partial x_j} \langle H_m, H_s, H_l \rangle + \frac{\partial p_m}{\partial x_i} \langle H_m, H_l \rangle - \frac{\partial}{\partial x_j} \left[\nu \left(\frac{\partial v_{jm}}{\partial x_i} + \frac{\partial v_{im}}{\partial x_j} \right) \right] \langle H_m, H_l \rangle = 0 \end{aligned} \tag{8}$$

where $l \in [0, L-1]$. For instance starting from eqs. (1), for $M = 1$ and $\gamma = 2$ (in which

case L=3), eqs. (8) give rise to 9 PDEs (to be solved for p_l, v_l) as follows

$$
\begin{aligned}
&{}^{l}R^{p} = -\frac{\partial v_{il}}{\partial x_i} = 0, \quad l = 0,1,2 \\
&{}^{0}R_i^{v} = v_{j0}\frac{\partial v_{i0}}{\partial x_j} + v_{j1}\frac{\partial v_{i1}}{\partial x_j} + 2v_{j2}\frac{\partial v_{i2}}{\partial x_j} + \frac{\partial p_0}{\partial x_i} - \frac{\partial}{\partial x_j}\left[\nu\left(\frac{\partial v_{j0}}{\partial x_i} + \frac{\partial v_{i0}}{\partial x_j}\right)\right] = 0 \\
&{}^{1}R_i^{v} = v_{j1}\frac{\partial v_{i0}}{\partial x_j} + v_{j0}\frac{\partial v_{i1}}{\partial x_j} + 2v_{j1}\frac{\partial v_{i2}}{\partial x_j} + 2v_{j2}\frac{\partial v_{i1}}{\partial x_j} + \frac{\partial p_1}{\partial x_i} - \frac{\partial}{\partial x_j}\left[\nu\left(\frac{\partial v_{j1}}{\partial x_i} + \frac{\partial v_{i1}}{\partial x_j}\right)\right] = 0 \\
&{}^{2}R_i^{v} = 4v_{j2}\frac{\partial v_{i2}}{\partial x_j} + v_{j1}\frac{\partial v_{i1}}{\partial x_j} + v_{j2}\frac{\partial v_{i0}}{\partial x_j} + v_{j0}\frac{\partial v_{i2}}{\partial x_j} + \frac{\partial p_2}{\partial x_i} - \frac{\partial}{\partial x_j}\left[\nu\left(\frac{\partial v_{j2}}{\partial x_i} + \frac{\partial v_{i2}}{\partial x_j}\right)\right] = 0
\end{aligned}
\tag{9}
$$

The expansions of the uncertain flow variables are introduced into the QoI in order to compute the PCE fields of the QoI. These are

$$
F_l = \int_S \left(-\nu\left(\frac{\partial v_{il}}{\partial x_j} + \frac{\partial v_{jl}}{\partial x_i}\right)n_j + p_l n_i \right) r_i dS, \qquad l \in [0, L-1] \tag{10}
$$

These coefficients are necessary in order to compute the mean value and standard deviation of the QoI, which are

$$
\mu_F = F_0, \qquad \sigma_F = \sqrt{\sum_{l=1}^{L-1} F_i \langle H_i, H_l \rangle} \tag{11}
$$

For $M=1$ and $\gamma=2$, $\sigma_F = \sqrt{F_1^2 + 2F_2^2}$. The cost of solving eqs. (8) and computing μ_F and σ_F is L EFS.

3.3 Assessment of the UQ using the MoM and iPCE

As already mentioned, the case examined is an isolated airfoil in a laminar (Re=3000) flow. The farfield flow angle has a mean value $\mu_{\alpha_\infty} = 4^o$ and a standard deviation $\sigma_{\alpha_\infty} = 0.3^o$. The volumetric B-Splines control box depicted in fig. 1 was used to parameterize the airfoil and the surrounding grid. In order to validate the UQ results, 3000 CFD evaluations were first performed with the MC method. The μ_F and σ_F of the drag (QoI), computed by the expensive MC, are considered as reference values. The statistical moments computed with the FOSM and iPCE are then compared with the reference values, table 1. Both methods estimate μ_F and σ_F with excellent accuracy (error less than 0.09% for μ_F and 0.69% for σ_F).

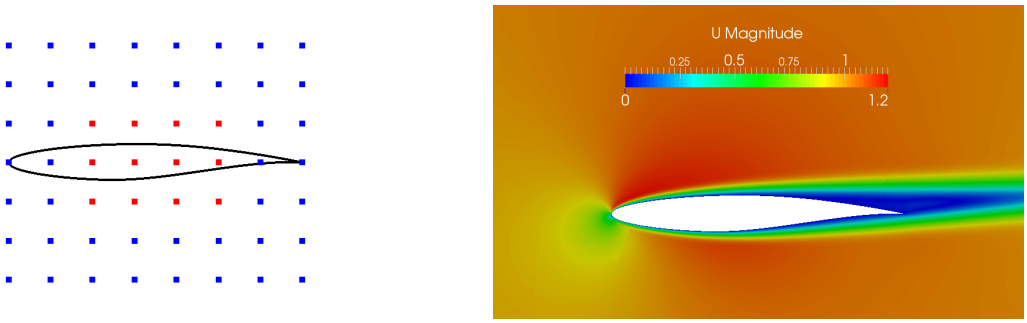

Figure 1: Initial airfoil shape and control box, with the active control points colored in red and inactive in blue (left); velocity magnitude iso-areas in the case without uncertainties (right).

Table 1: Comparison of the mean value and standard deviation of the QoI (drag) computed using the MC, FOSM and iPCE.

	MC	FOSM	iPCE
μ_F	0.034999	0.035030	0.035003
σ_F	$1.5401{\cdot}10^{-4}$	$1.5507{\cdot}10^{-4}$	$1.5340{\cdot}10^{-4}$

4 Gradient Computation and Optimization

4.1 Method of Moments (MoM)

A gradient-based shape optimization requires the computation of $\frac{\delta J}{\delta b_n}$, where b_n, $n \in [1, N]$ are the design variables. The differentiation of eq. (3) gives

$$\frac{\delta J}{\delta b_n} = w_0 \frac{\delta F}{\delta b_n} + w_1 \frac{\sum_{\mu=1}^{M} \frac{\delta F}{\delta c_\mu} \frac{\delta^2 F}{\delta c_\mu \delta b_n} \sigma_\mu^2}{\sqrt{\sum_{\mu=1}^{M} \left[\frac{\delta F}{\delta c_\mu}\right]^2 \sigma_\mu^2}} = w_0 \frac{\delta F}{\delta b_n} + w_1 \frac{\sum_{\mu=1}^{M} \frac{\delta^2 F}{\delta c_\mu \delta b_n} z_\mu}{\sqrt{\sum_{\mu=1}^{M} \left[\frac{\delta F}{\delta c_\mu}\right]^2 \sigma_\mu^2}} \tag{12}$$

where $z_\mu = \{\frac{\delta F}{\delta c_\mu} \sigma_\mu^2\}$ is a vector; curly brackets indicate no summation over the repeated index. In order to avoid any misinterpretation of the more than twice repeated index μ, in eq. (12) the summation symbol is used. To compute $\frac{dJ}{db_n}$, it is necessary to compute three different groups of derivatives, specifically

$$\frac{\delta F}{\delta b_n}, \quad \sum_{\mu=1}^{M} \left[\frac{\delta F}{\delta c_\mu}\right]^2 \sigma_\mu^2, \quad \sum_{\mu=1}^{M} \frac{\delta^2 F}{\delta c_\mu \delta b_n} \frac{\delta F}{\delta c_\mu} \sigma_\mu^2$$

All first-order derivatives can be computed from the solution of the same continuous adjoint equations, section (3.1). The second term is known from eq. (6) whereas the first of them results from

$$\frac{\delta F}{\delta b_n} = \int_\Omega A_{jk} \frac{\partial}{\partial x_j}\left(\frac{\delta x_k}{\delta b_n}\right) d\Omega + \int_{S_w} \left(p\delta_i^j - \tau_{ij}\right) r_i \frac{\delta\left(n_j dS\right)}{\delta b_n} \tag{13a}$$

$$A_{jk} = q\frac{\partial v_j}{\partial x_k} - u_i v_j \frac{\partial v_i}{\partial x_k} - \tau_{ij}^a \frac{\partial v_i}{\partial x_k} + u_i \frac{\partial \tau_{ij}}{\partial x_k} - u_j \frac{\partial p}{\partial x_k} \tag{13b}$$

The third term includes the second-order derivatives $\frac{\delta^2 F}{\delta c_\mu \delta b_n}$, to be referred to as mixed $b-c$ derivatives, multiplied by the vector $\vec{z}$. The concept of the pFOSM is inspired from the truncated Newton technique presented in [4]. Instead of separately computing all $\frac{\delta^2 F}{\delta c_\mu \delta b_n}$ derivatives and, then, performing the contraction with z_μ, it is proposed to directly compute the projection of the projected $b-c$ mixed derivatives onto $\vec{z}$.

Computing $\frac{\delta^2 F}{\delta c_\mu \delta b_n}$ through a combination of adjoint and direct differentiation would have a cost that scales with M, [6]. Instead, eq. (13a) is differentiated w.r.t. c_μ and the result is projected onto $\vec{z}$. The final expression for the b-c mixed derivatives is

$$\begin{aligned}\frac{\delta^2 F}{\delta c_\mu \delta b_n} z_\mu = \int_\Omega \Bigg(& \tilde{q}\frac{\partial v_j}{\partial x_k} + q\frac{\partial \tilde{v_j}}{\partial x_k} - v_j\tilde{u_i}\frac{\partial v_i}{\partial x_k} - u_i\tilde{v_j}\frac{\partial v_i}{\partial x_k} - u_i v_j \frac{\partial \tilde{v_i}}{\partial x_k} - \tilde{\tau}_{ij}^a \frac{\partial v_i}{\partial x_k} - \tau_{ij}^a \frac{\partial \tilde{v_i}}{\partial x_k} \\ & + \tilde{u_i}\frac{\partial \tau_{ij}}{\partial x_k} + u_i \frac{\partial \tilde{\tau}_{ij}}{\partial x_k} - \tilde{u_j}\frac{\partial p}{\partial x_k} - u_j \frac{\partial \tilde{p}}{\partial x_k}\Bigg) \frac{\partial}{\partial x_j}\left(\frac{\delta x_k}{\delta b_n}\right) d\Omega + \int_{S_w} \left(\tilde{p}\delta_i^j - \tilde{\tau}_{ij}\right) r_i \frac{\delta\left(n_j dS\right)}{\delta b_n}\end{aligned} \tag{14}$$

where the ($\tilde{}$) symbol is used for the projected derivatives of the primal and adjoint variables (e.g. $\tilde{v_i} = \frac{\delta v_i}{\delta c_\mu} z_\mu$, etc.).

Hence, only the projected derivatives have to be computed, instead of the M fields (such as $\frac{\delta v_i}{\delta c_\mu}, \mu \in [1, M]$, etc.). The projected fields can be computed by differentiating eqs. (1) and (5) w.r.t. c_μ and projecting the result onto $\vec{z}$, i.e. by solving

$$\begin{aligned}
\tilde{R^p} &= -\frac{\delta R^p}{\delta c_\mu} z_\mu = -\frac{\partial \tilde{v_j}}{\partial x_j} = 0 \\
\tilde{R_i^v} &= \frac{\delta R_i^v}{\delta c_\mu} z_\mu = \tilde{v_j}\frac{\partial v_i}{\partial x_j} + v_j \frac{\partial \tilde{v_i}}{\partial x_j} - \frac{\partial \tilde{\tau}_{i,j}}{\partial x_j} + \frac{\partial \tilde{p}}{\partial x_i} = 0, \quad i = 1, 2 \\
\tilde{R^q} &= \frac{\delta R^q}{\delta c_\mu} z_\mu = -\frac{\partial \tilde{u_j}}{\partial x_j} = 0 \\
\tilde{R_i^u} &= \frac{\delta R^u}{\delta c_\mu} z_\mu = \tilde{u_j}\frac{\partial v_j}{\partial x_i} + u_j \frac{\partial \tilde{v_j}}{\partial x_i} - \tilde{v_j}\frac{\partial u_i}{\partial x_j} - v_j \frac{\partial \tilde{u_i}}{\partial x_j} - \frac{\partial \tilde{\tau}_{i,j}^a}{\partial x_j} + \frac{\partial \tilde{q}}{\partial x_i} = 0, \quad i = 1, 2
\end{aligned} \tag{15}$$

After solving eqs. (15) for $\tilde{v_i}$, $\tilde{u_i}$, $\tilde{p}$, $\tilde{q}$, the projected $b-c$ mixed derivatives are computed through eq. (14) at a negligible CPU cost. The total cost of pFOSM is 4 EFS per cycle, independent of the M and N values.

The three groups of derivatives necessary for the final computation of the sensitivity derivatives, i.e. $\frac{\delta F}{\delta c_\mu}$, $\frac{\delta F}{\delta b_n}$ and $\frac{\delta^2 F}{\delta c_\mu \delta b_n} z_\mu$, with $c_\mu = \alpha_\infty$, are validated against Finite Differences

(FD). Regarding $\frac{\delta F}{\delta a_\infty}$, its value is computed equal to -0.02919 with FD and -0.02973 using adjoint; their difference in value is less than 2%. The validation of the other two groups of derivatives is presented in fig. 2. Based on eq. (12), $\frac{\delta J}{\delta b_n}$ has been exactly computed.

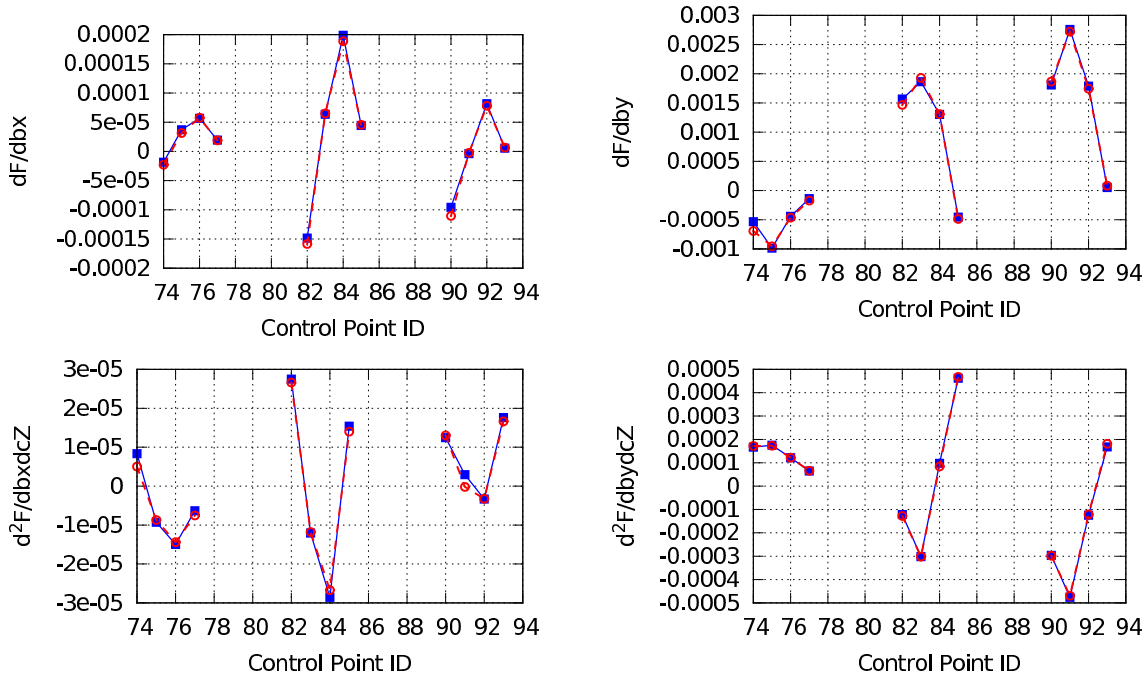

Figure 2: Results obtained with FD (blue filled squares) and the method of section 4.1 (red empty circles) for $\frac{dF}{db_n}$ (top) and $\frac{\delta^2 F}{\delta c_\mu \delta b_n} z_\mu$ (bottom), where $c_\mu = \alpha_\infty$.

4.2 Continuous Adjoint to the iPCE

Having formulated and validated the iPCE equations (eqs. (9) for $M = 1$, $\gamma = 2$), the next step is to compute the gradient of the objective function w.r.t. the design variables ($\frac{dJ}{db_n}$). To this end, the continuous adjoint method is also used; thus, new field adjoint equations should be formulated along with their boundary conditions and sensitivity derivative expressions. The cost of solving the adjoint equations is L EFS; hence, for the optimization loop, the total cost per cycle is $2L$ EFS (6 EFS for $M = 1$, $\gamma = 2$). The augmented objective function is

$$J_{aug} = J + \int_\Omega \left({}^0R_i^v u_{i0} + {}^0R^p q_0 + {}^1R_i^v u_{i1} + {}^1R^p q_1 + {}^2R_i^v u_{i2} + {}^2R^p q_2 \right) d\Omega \tag{16}$$

where u_{il} and q_l are the adjoint iPCE velocity and pressure fields, respectively. The continuous adjoint development results to the system of field adjoint equations

$$\begin{aligned}
&\frac{\partial u_{il}}{\partial x_i} = 0, \quad l = 0, 1, 2 \\
&u_{j0}\frac{\partial v_{j0}}{\partial x_i} + u_{j1}\frac{\partial v_{j1}}{\partial x_i} + 2u_{j2}\frac{\partial v_{j2}}{\partial x_i} - \frac{\partial}{\partial x_j}\left(u_{i0}v_{j0} + u_{i1}v_{j1} + 2u_{i2}v_{j2}\right) + \frac{\partial q_0}{\partial x_i} - \frac{\partial \tau^a_{ij0}}{\partial x_j} = 0 \\
&u_{j1}\frac{\partial v_{j0}}{\partial x_i} + u_{j0}\frac{\partial v_{j1}}{\partial x_i} + 2u_{j1}\frac{\partial v_{j2}}{\partial x_i} + 2u_{j2}\frac{\partial v_{j1}}{\partial x_i} - \frac{\partial}{\partial x_j}\left(u_{i1}v_{j0} + u_{i0}v_{j1} + 2u_{i1}v_{j2} + 2u_{i2}v_{j1}\right) + \frac{\partial q_1}{\partial x_i} - \frac{\partial \tau^a_{ij1}}{\partial x_j} = 0 \\
&4u_{j2}\frac{\partial v_{j2}}{\partial x_i} + u_{j1}\frac{\partial v_{j1}}{\partial x_i} + u_{j0}\frac{\partial v_{j2}}{\partial x_i} + u_{j2}\frac{\partial v_{j0}}{\partial x_i} - \frac{\partial}{\partial x_j}\left(4u_{i2}v_{j2} + u_{i1}v_{j1} + u_{i0}v_{j2} + u_{i2}v_{j0}\right) + \frac{\partial q_2}{\partial x_i} - \frac{\partial \tau^a_{ij2}}{\partial x_j} = 0
\end{aligned} \tag{17}$$

where τ^a_{ijk} is the adjoint stress tensor of the k^{th} iPCE field. At the inlet boundary, zero Dirichlet conditions are imposed to u_i and a zero Neumann condition to q_i. Along the parameterized walls, a zero Neumann is imposed to q_i whereas $u_0 = -w_0 r_i$, $u_1 = -\frac{w_1 F_1 r_i}{\sqrt{(F_1^2+2F_2^2)}}$, $u_2 = -\frac{2w_1 F_2 r_i}{\sqrt{(F_1^2+2F_2^2)}}$ where F_l are given by eq. (10). Finally, for the outlet, $q_l = u_i^n v_j^n \langle H_i, H_j, H_l\rangle + 2\nu \frac{\partial u_i^n}{\partial n}\langle H_i, H_l\rangle$, and $v_i^n u_j^t \langle H_i, H_j, H_l\rangle + \nu(\frac{\partial u_i^t}{\partial n} + \frac{\partial u_i^n}{\partial t})\langle H_i, H_l\rangle = 0$, where superscripts n, t stand for the normal and the tangential velocity component, respectively.

Once eqs. (17) have been solved, the sensitivity derivatives are computed by

$$\begin{aligned}
\frac{\delta J}{\delta b_n} = &\int_{Sw}\left(w_0(-\tau_{ij0} + p_0\delta_i^j) + \frac{w_1 F_1(-\tau_{ij1} + p_1\delta_i^j)}{\sqrt{F_1^2+2F_2^2}} + \frac{2w_1 F_2(-\tau_{ij2} + p_2\delta_i^j)}{\sqrt{F_1^2+2F_2^2}}\right) r_i \frac{\delta(n_j dS)}{\delta b_n} \\
&- \int_\Omega \Bigg[\left(u_{i0}v_{j0} + u_{i1}v_{j1} + 2u_{i2}v_{j2} + \tau^a_{ij0} - q_0\right)\frac{\partial v_{i0}}{\partial x_k} + \Bigg(u_{i0}v_{j1} + u_{i1}v_{j0} + 2u_{i1}v_{j2} + \\
&2u_{i2}v_{j1} + \tau^a_{ij1} - q_1\Bigg)\frac{\partial v_{i1}}{\partial x_k} + \left(8u_{i2}v_{j2} + 2u_{i1}v_{j1} + 2u_{i2}v_{j0} + 2u_{i0}v_{j2} + 2\tau^a_{ij2} - 2q_2\right)\frac{\partial v_{i2}}{\partial x_k} \\
&+ u_{j0}\frac{\partial p_0}{\partial x_k} + u_{j1}\frac{\partial p_1}{\partial x_k} + 2u_{j2}\frac{\partial p_2}{\partial x_k} - u_{i0}\frac{\partial \tau_{ij0}}{\partial x_k} - u_{i1}\frac{\partial \tau_{ij1}}{\partial x_k} - 2u_{i2}\frac{\partial \tau_{ij2}}{\partial x_k}\Bigg]\frac{\partial}{\partial x_j}\left(\frac{\delta x_k}{\delta b_n}\right)
\end{aligned} \tag{18}$$

The sensitivity derivatives computed through eq. (18) are validated against FD, fig. 3. Two extreme sets of weights were used ((w_0, w_1) = (1,0) and (0,1)), and the derivatives of both are in close agreement with FD.

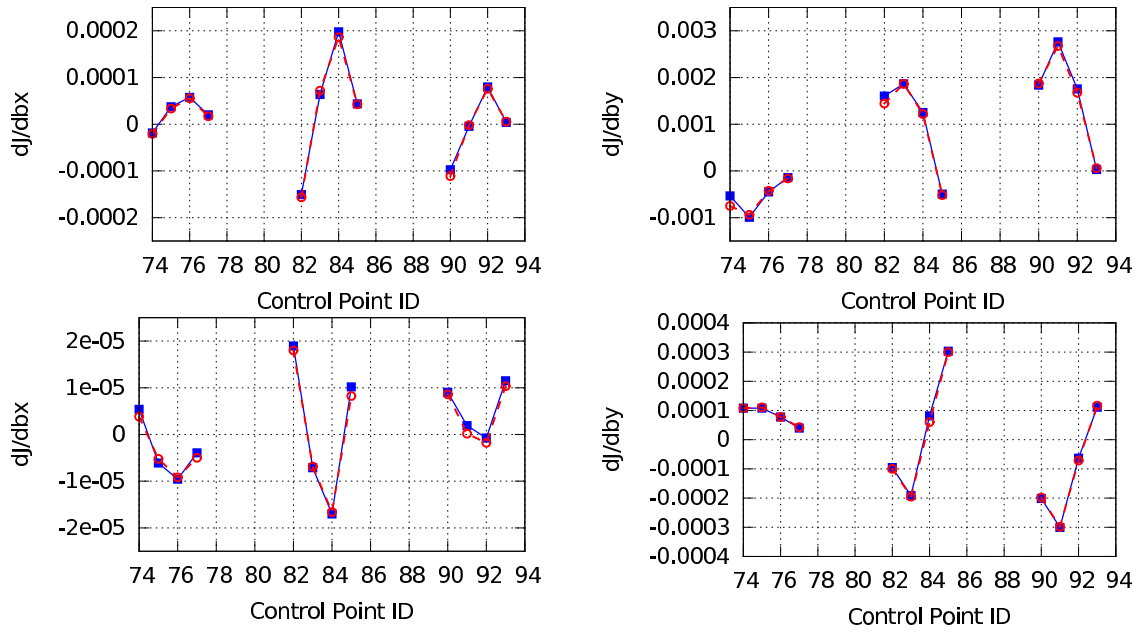

Figure 3: $\frac{dJ}{db_n}$ computed with FD (blue filled squares) and the adjoint iPCE (red empty circles) for (w_0,w_1)=(1,0) (top) and (w_0,w_1)=(0,1) (bottom).

4.3 Optimization Results

A number of optimization runs with different value-sets of (w_0, w_1) were performed in order to form the Pareto front of non-dominated solutions, on the (μ_F,σ_F) plane, fig. 4. All optimization runs were conducted under the constraint of constant airfoil volume, implemented through the constraint projection method,

$$\frac{\delta J'}{\delta b_n} = \frac{\delta J}{\delta b_n} - \frac{\left(\frac{\delta J}{\delta b_k}\frac{\delta V}{\delta b_k}\right)\frac{\delta V}{\delta b_n}}{\frac{\delta V}{\delta b_n}^2}, \qquad \frac{\delta V}{\delta b_n} = \int_{S_w} \frac{\delta x_k}{\delta b_n} n_k dS \tag{19}$$

For the cases with weights (w_0, w_1)=(1,6) and (1,7), the final geometry has both μ_F and σ_F improved, which is a very desirable feature. In general, the results of both methods are quite similar and the optimization had a great impact on the σ_F reduction (up to 80% reduction). The initial and final optimized shapes produced by iPCE and pFOSM for weights (1,0) and (0,1) are presented in fig. 5. Due to the volume constraint displacements are limited, making it impossible to present all geometries in the same figure; these are, though bounded by the green and red contours.

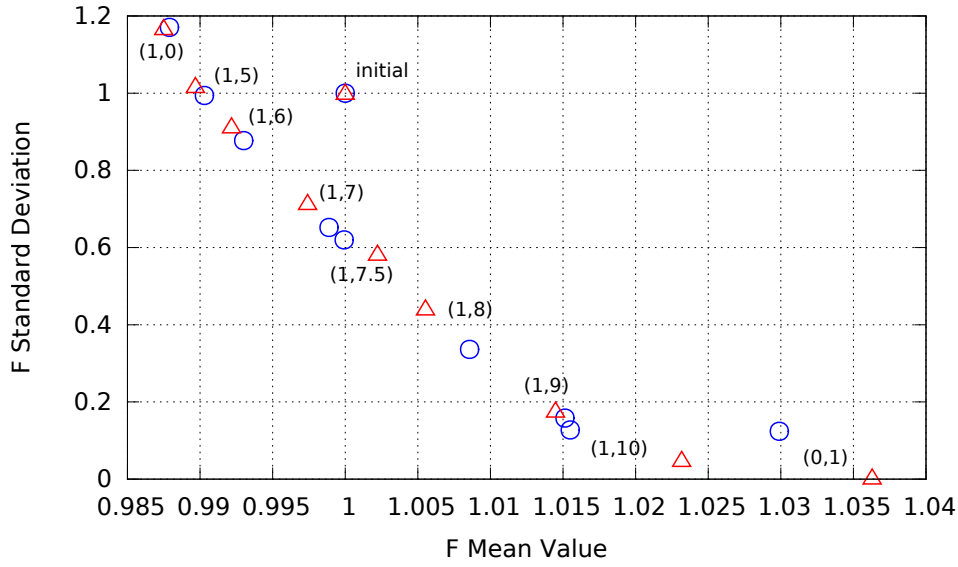

Figure 4: Pareto front on the (μ_F, σ_F) plane. All values are normalized with those of the initial geometry (circles computed by the iPCE, triangles by the pFOSM).

Figure 5: Comparison of the initial (red curve), μ_F optimal (blue curve) and σ_F optimal (green curve) geometries designed by the pFOSM (left) and the iPCE (right).

5 Summary - Conclusions

This paper presents two different methods for quantifying uncertainty in incompressible flows, namely the FOSM and the iPCE. For the problem examined, the results concerning UQ were absolutely satisfactory for both methods, even if the former is a first-order one. Both require the development of additional equations and solvers though, for the former, the adjoint solver was already available.

Regarding aerodynamic shape optimization under uncertainties, workflows based on the continuous adjoint to compute the gradients of the FOSM- and iPCE-based UQ metrics are presented and validated against FD. The adjoint to the iPCE equations and a novel method for computing the projected second-order derivatives (the pFOSM approach), emerging when using the FOSM in a gradient-based optimization, were developed for the first time in the literature (at least to the authors knowledge); the latter led to the developed of a robust design algorithm with a cost that does not scale with either the number of design or uncertain variables. Applying the developed methods for minimizing the weighted sum of the mean value and standard deviation of the drag force exerted on

an airfoil led to a Pareto front of non-dominated solutions; the cost per optimization cycle along with the cost for the UQ is summarized in table 2. Extension of both methods to turbulent flows and the development of a second-order MoM (SOSM), are in progress.

Table 2: Computational cost for the UQ and optimization with the pFOSM and iPCE methods, for M uncertain variables.

	UQ (EFS)	Optimization Cycle (EFS)
pFOSM	2	4
iPCE	$\frac{1}{2}(M^2+3M+2)$	M^2+3M+2

REFERENCES

[1] C. Dinescu, S. Smirnov, C. Hirsch, and C. Lacor. Assessment of intrusive and non-intrusive non-deterministic CFD methodologies based on polynomial chaos expansion. *International Journal of Engineering Systems Modeling and Simulations*, 2:87–98, 2010.

[2] C. Lacor, C. Dinescu, C. Hirsch, and S. Smirnov. *Implementation of intrusive polynomial chaos in CFD codes and application to 3D Navier-Stokes.* Springer International Publishing, 2013.

[3] W. Morokoff and R. Caflisch. Quasi-Monte Carlo integration. *Journal of Computational Physics*, 122(2):218 – 230, 1995.

[4] D. Papadimitriou and K. Giannakoglou. Aerodynamic design using the truncated Newton algorithm and the continuous adjoint approach. *International Journal for Numerical Methods in Fluids*, 68(6):724–739, 2012.

[5] E. Papoutsis-Kiachagias and K. Giannakoglou. Continuous adjoint methods for turbulent flows, applied to shape and topology optimization: Industrial applications. *Archives of Computational Methods in Engineering*, 23(2):255–299, 2016.

[6] E. Papoutsis-Kiachagias, D. Papadimitriou, and K. Giannakoglou. Robust design in aerodynamics using 3rd-order sensitivity analysis based on discrete adjoint. Application to quasi-1D flows. *International Journal for Numerical Methods in Fluids*, 69(3):691–709, 2012.

[7] D. Xiu and J. Hesthaven. High-order collocation methods for differential equations with random inputs. *SIAM J. Sci. Comput.*, 27:1118–1139, 2005.

[8] D. Xiu and GM. Karniadakis. Modeling uncertainty in flow simulations via generalized polynomial chaos. *Journal of Cimputational Physics*, 187:137–167, 2003.